Electron-impact excitation of oxygenlike krypton

Alfred Z. Msezane and J. Lee
Department of Physics, Atlanta University, Atlanta, Georgia 30314

Kennedy J. Reed
V-Division, Lawrence Livermore National Laboratory, Livermore, California 94550

Ronald J. W. Henry
Department of Physics and Astronomy, Louisiana State University, Baton Rouge, Louisiana 70803
(Received 21 April 1986)

Electron-impact excitation cross sections have been calculated for transitions from the ground state $2s^2 2p^4\,{}^3P$ to the $n=2$ and $n=3$ excited states of oxygenlike krypton. Configuration-interaction-type wave functions were employed, and the cross sections were calculated in a close-coupling approximation for impact energies ranging from near threshold to 10 keV. Coupling between the $n=2$ and $n=3$ excitation levels was generally found to be weak, and a two-state close-coupling approximation should be adequate for calculating reliable cross sections for most transitions.

I. INTRODUCTION

Ions of oxygenlike sequence are of interest for astrophysics and for studies of plasmas produced in laboratory experiments. Feldman and Doschek[1] have determined that intensity ratios of certain spectral emission lines from oxygenlike ions may be sensitive to electron density for a wide range of temperatures and thus may be useful for purposes of plasma diagnostics. In order to properly interpret information obtained from spectral lines emitted from plasmas, accurate energy levels, oscillator strengths, and electron collision cross sections are needed. Calculations and measurements of energy levels and oscillator strengths for oxygenlike ions have been reported by several authors.[2–4] Because of the difficulties of measuring electron-ion excitation cross sections, very few such measurements have been reported for ions of any sequence. The codes which are used to model laboratory plasmas require cross sections for large numbers of transitions and users of these codes rely heavily upon calculated cross sections for studies of plasma parameters. However, accurate electron collision cross sections are also difficult to calculate and relatively few such calculations have been reported for ions of intermediate and high atomic number.

We report calculations of electron-impact excitation cross sections for some transitions in oxygenlike krypton. Emission lines from this ion may be used as a density diagnostic in high-temperature tokamak plasmas. Our calculations are motivated in part by observations of oxygenlike krypton in plasmas produced in experiments on a gas-puff Z-pinch machine.[5] Bhatia and Feldman[6] have reported electron collision strengths for transitions among the $2s^2 2p^4$, $2s2p^5$, and $2p^6$ configurations of oxygenlike krypton. Their calculations were done in a distorted-wave approximation using the computer package developed at the University College, London. Our calculations are carried out in a multistate close-coupling approximation and include transitions from the ground state $2s^2 2p^4\,{}^3P$ to all of the $n=2$ and $n=3$ excited states of the ion. Only a few representative results in LS coupling are reported here. In a separate paper we discuss close-coupling cross sections in intermediate coupling for transitions from the ground state to $n=2$ excited states of Kr^{+28},[7] and in that paper we compare our results to the distorted-wave results of Bhatia and Feldman.

It has been shown that the accuracy of electron collisional excitation cross sections is very sensitive to the representation of the target wave function and to the strength of the couplings between the various channels.[8] However, for inner-shell excitation of multicharged ions, it appears that the scattering approximation is more important than a sophisticated target wave function.[9,10] We used configuration-interaction-type target wave functions which we constructed after the extensive testing of the effects of configuration interaction upon the oscillator strengths and energy levels of the target states. In generating the $3s$, $3p$, and $3d$ orbitals, we required that oscillator strengths calculated in the dipole length and velocity approximations agree reasonably well with each other. We studied the effects of couplings among the terms of the ground-state configuration by including the $2s^2 2p^4\,{}^1D$ and $2s^2 2p^4\,{}^1S$ terms along with the $2s^2 2p^4\,{}^3P$ and we tested the effects of couplings among some excited states as well. We also discuss some partial cross sections as a function of L as well as the energy dependence of certain partial cross sections.

In Secs. II and III we present the calculational procedure and the results, respectively. Discussion and conclusions are given in Sec. IV.

II. PROCEDURE

Hartree-Fock orbitals of Clementi and Roetti[11] were used as a starting point for the $1s$, $2s$, and $2p$ orbitals for the ground state of the target ion. Hibbert's program CIV3 (Ref. 12) was used to generate the excited $3s$, $3p$, $3d$, $4s$,

 ©1986 The American Physical Society

TABLE I. Coefficients and exponents for some orbitals for Kr^{+28}. The radial functions are given by

$$P_{nl}(r)=r^l\sum_{i=1}^{(n-l)} a_i r^i e^{-\alpha_i r} .$$

nl	a_1	a_2	a_3	a_4	α_1	α_2	α_3	α_4
$3s$	68.336 04	−1075.530 56	1736.324 57	0.0	18.841 69	14.022 16	9.601 97	0.0
$3p$	225.121 74	−284.993 37	0.0	0.0	12.634 60	6.253 94	0.0	0.0
$3d$	571.185 62	0.0	0.0	0.0	7.848 94	0.0	0.0	0.0
$4s$	14.128 18	−323.357 34	76.415 09	−27.127 06	16.968 10	19.703 29	6.236 95	3.309 57
$4p$	77.180 88	−106.249 59	14.742 85	0.0	12.555 00	6.067 80	2.896 12	0.0
$4d$	70.880 99	−27.645 33	0.0	0.0	5.782 41	3.300 30	0.0	0.0

$4p$, $4d$, and $5s$ orbitals, and to obtain configuration-interaction (CI) wave functions for all states in the LS coupling scheme. The wave functions are of the form

$$\Psi(LS)=\sum_{i=1}^{N} c_i\varphi_i(\beta_i LS) , \tag{1}$$

where the single-configuration functions φ_i are constructed from one-electron orbitals. Each orbital consists of a product of a spin function, a spherical harmonic, and a radial function. The angular momenta are coupled in a manner prescribed by (β_i) to give the total orbital and spin angular momenta L and S, respectively.

The radial functions of the orbital are given by

$$P_{nl}(r)=r^l\sum_{i=1}^{(n-l)} a_i r^i e^{-\alpha_i r} , \tag{2}$$

where n and l are the principal and orbital angular momentum quantum numbers. For a given choice of exponents, α_i, the expansion coefficients, a_i, are uniformly determined from the orthogonality condition

$$\int_0^\infty P_{nl}(r)P_{n'l}(r)dr=\delta_{nn'} , \quad l\le n'\le n . \tag{3}$$

The excited-state orbitals were constructed and energy optimized one at a time using CIV3 according to Eq. (3). In

TABLE II. Some energy levels for Kr^{+28}.

i	Level	Configuration	ΔE (a.u.)
1	^3P	$2s^22p^4$	0.0
2	^1D	$2s^22p^4$	0.6759
3	^1S	$2s^22p^4$	1.4319
4	$^3P^\circ$	$2s2p^5$	5.4703
5	$^1P^\circ$	$2s2p^5$	7.4698
6	^1S	$1s^22p^6$	12.8449
7	$^5S^\circ$	$2s^22p^3 3s$	66.1490
8	$^3S^\circ$	$2s^22p^3 3s$	66.5444
9	$^3D^\circ$	$2s^22p^3(^2D)3s$	67.2730
10	$^1D^\circ$	$2s^22p^3(^2D)3s$	67.4698
11	$^3P^\circ$	$2s^22p^3 3s$	67.7675
12	$^1P^\circ$	$2s^22p^3 3s$	67.9607
13	^5P	$2s2p^4 3s$	70.7113
14	^1P	$2s2p^4(^3P)3s$	71.2552
15	^3P	$2s2p^4(^3P)3s$	71.2801
16	$^5D^\circ$	$2s^22p^3(^4S)3d$	72.0562
17	$^3D^\circ$	$2s^22p^3(^1S)3d$	72.2822
18	^3D	$2s2p^4(^1D)3s$	72.4568
19	^1D	$2s2p^4(^1D)3s$	72.9614
20	$^1S^\circ$	$2s^22p^3(^2D)3d$	73.0033
21	$^3F^\circ$	$2s^22p^3(^2D)3d$	73.0686
22	$^3G^\circ$	$2s^22p^3 3d$	73.1319
23	$^3D^\circ$	$2s^22p^3(^2D)3d$	73.1626
24	$^1G^\circ$	$2s^22p^3 3d$	73.1652
25	$^1P^\circ$	$2s^22p^3 3d$	73.1982
26	$^1D^\circ$	$2s^22p^3(^2D)3d$	73.2577
27	$^3D^\circ$	$2s^22p^3(^2D)3d$	73.2980
28	$^3S^\circ$	$2s^22p^3 3d$	73.3209

TABLE II. (*Continued*).

i	Level	Configuration	ΔE (a.u.)
29	^3P	$2s2p^4 3s$	73.4479
30	$^1F^\circ$	$2s^2 2p^3(^2D)3d$	73.5307
31	$^3P^\circ$	$2s^2 2p^3(^2P)3d$	73.6573
32	$^3D^\circ$	$2s^2 2p^3(^2P)3d$	73.6758
33	$^1D^\circ$	$2s^2 2p^3(^2P)3d$	73.7348
34	$^3F^\circ$	$2s^2 2p^3(^2P)3d$	73.8154
35	^1S	$2s2p^4 3s$	73.9781
36	$^1F^\circ$	$2s^2 2p^3(^2P)3d$	74.0398
37	^5P	$2s^2 2p^3 3p$	74.0688
38	$^1P^\circ$	$2s^2 2p^3(^2P)3d$	74.1036
39	^1P	$2s^2 2p^3(^4S)3p$	74.1835
40	^3P	$2s^2 2p^3(^4S)3p$	74.2079
41	^1P	$2s^2 2p^3(^2D)3p$	74.0764
42	^3F	$2s^2 2p^3 3p$	75.1144
43	^3D	$2s^2 2p^3(^2D)3p$	75.1203
44	^1F	$2s^2 2p^3 3p$	75.1342
45	^3P	$2s^2 2p^3(^2D)3p$	75.2334
46	^1D	$2s^2 2p^3(^2D)3p$	75.3316
47	^3D	$2s^2 2p^3(^2P)3p$	75.5815
48	^1P	$2s^2 2p^3(^2P)3p$	75.6239
49	^3S	$2s^2 2p^3 3p$	75.6365
50	^3P	$2s^2 2p^3(^2P)3p$	75.6633
51	^1D	$2s^2 2p^3(^2P)3p$	75.6755
52	^1S	$2s^2 2p^3 3p$	75.8995
53	^5D	$2s2p^4(^3P)3d$	76.4462
54	^5P	$2s2p^4 3d$	76.7246
55	^3D	$2s[2p^4(^3P)]^4P3d$	76.9779

constructing the excited-state orbitals, the $1s^2$ core is frozen. The orbital parameters of the excited orbitals thus determined are given in Table I. In Table II we list some of the energy ordered levels along with the configurations and the energies relative to the ground state. These were obtained from set-I wave functions (described below) which yielded a ground-state energy of -2071.9332 a.u. for the ion.

The oscillator strengths in the length f_L and velocity f_V forms are given, respectively, by[12]

$$f_L=\frac{2\Delta E}{3g^{(i)}}\sum\left|\left\langle\Psi^{(i)}\left|\sum_j^N \mathbf{r}_j\right|\Psi^{(f)}\right\rangle\right|^2 \tag{4}$$

and

$$f_V=\frac{2}{3g^{(i)}\Delta E}\sum\left|\left\langle\Psi^{(i)}\left|\sum_j^N \nabla_j\right|\Psi^{(f)}\right\rangle\right|^2, \tag{5}$$

where the outer sum is over M_L and M_s degeneracies of the two states, and

$$\Delta E=E^{(f)}-E^{(i)},$$

$$g^{(i)}=(2L^{(i)}+1)(2S^{(i)}+1).$$

Superscripts (i) and (f) refer to initial and final states, respectively, N is the number of electrons, and E is the energy of the state.

Our target wave functions were initially constructed with configurations having orbitals with principal quantum number up to $n=5$ and $l=2$. In Table III two sets of results are presented for f_L and f_V and are designated by (i) and (ii). These were produced from target wave functions designated by I and II, respectively. Set (i) was obtained by using a target wave function for the ground state containing 12 configurations. The energy levels in Table II were obtained using this set. However, in order to reduce the enormous computer time required to calculate the cross sections, the set II was generated from set I by retaining only a single configuration for the ground state which yields a total energy of -2071.9171 a.u. for the ion. Configuration-interaction wave functions were employed to describe the excited states, except that for set II, only configurations containing orbitals with n up to 4 and $l=2$ were retained.

The program CIV3 was used to generate the CI coefficients for the configurations which describe the target wave functions. Initially, we included all the configurations of the same symmetry as the given target states and containing excited orbitals up to $n=4$ and $l=2$. Finally, the number of terms in the expansion of the target wave functions was reduced by retaining only CI coefficients which are greater than 5×10^{-5}. Table IV gives the CI coefficients for some of the set-II target wave functions employed in the calculation of the cross sections.

The reduction from set-I to set-II wave functions did not alter the f values significantly, as can be seen by comparing results (i) and (ii) in Table III. In addition, tests

TABLE III. Oscillator strengths for Kr^{+28}. The figure in square brackets is the power of 10 by which the number is multiplied.

		(i)			(ii)	
Level	Configuration	f_L	f_V	ΔE (a.u.)	f_L	f_V
$^3S^\circ$	$2s^22p^33s$	0.272[−1]	0.271[−1]	66.5459	0.268[−1]	0.270[−1]
	$2s^22p^33d$	0.136	0.100	73.3149	0.134	0.100
	$2s\,2p^4(^4P)3p$	0.186[−1]	0.954[−2]	78.3232	0.179[−1]	0.950[−2]
	$2s\,2p^4(^2P)3p$	0.725[−2]	0.352[−2]	81.3214	0.736[−2]	0.353[−2]
	$2s^22p^34s$	0.557[−3]	0.548[−3]			
	$2s^22p^34d$	0.211[−2]	0.913[−3]			
	$2s2p^44p$	0.109[−3]	0.763[−4]			
	$2s^22p^2(^3P)3s\,3p$	0.777[−3]	0.288[−3]			
$^3P^\circ$	$2s2p^5$	0.612[−1]	0.487[−1]	5.4642	0.616[−1]	0.438[−1]
	$2s^22p^33s$	0.214[−1]	0.225	67.7625	0.220[−1]	0.224[−1]
	$2s^22p^3(^2D)3d$	0.371	0.273	73.2920	0.355	0.273
	$2s^22p^3(^2P)3d$	0.319[−1]	0.239[−1]	73.6521	0.333[−1]	0.240[−1]
	$2p^53s$	0.123[−1]	0.700[−2]	78.2293	0.118[−1]	0.697[−2]
	$2s2p^4(^4P)3p$	0.455	0.232[−1]	78.8479	0.428[−1]	0.230[−1]
	$2s2p^4(^2P)3p$	0.196[−1]	0.923[−2]	81.6124	0.195[−1]	0.921[−2]
	$2p^53d$	0.480[−3]	0.560[−3]	83.9259	0.762[−3]	0.580[−3]
	$2s^22p^34s$	0.320[−3]	0.210[−3]			
$^3D^\circ$	$2s^22p^3(^2D)3s$	0.387[−1]	0.381[−1]	67.2686	0.384[−1]	0.377[−1]
	$2s^22p^3(^4S)3d$	0.308	0.233	72.3384	0.301	0.232
	$2s^22p^3(^2D)3d$	0.395	0.302	73.2193	0.393	0.296
	$2s^22p^3(^2P)3d$	0.367	0.276	73.7347	0.366	0.271
	$2s2p^4(^3P)3p$	0.803[−1]	0.403[−1]	78.6649	0.771[−1]	0.401[−1]
	$2s2p^4(^1D)3p$	0.200[−3]	0.100[−4]	80.3572	0.230[−4]	0.140[−4]
	$2s2p^4(^3P)3p$	0.413[−1]	0.201[−1]	81.5898	0.396[−1]	0.191[−1]
	$2p^53d$	0.283[−2]	0.202[−2]	84.1910	0.297[−2]	0.188[−2]
	$2s^22p^3(^2D)4s$	0.490[−3]	0.370[−3]			
	$2s^22p^3(^4S)4d$	0.794[−3]	0.371[−3]			
	$2s^22p^3(^2D)4d$	0.388[−2]	0.164[−2]			
	$2s^22p^3(^2P)3d$	0.492[−2]	0.199[−2]			
	$2s2p^4(^3P)3p$	0.187[−2]	0.670[−3]			

TABLE IV. Some CI coefficients for Kr^{+28}.

$$2p^6\,{}^1S = -0.15385(2s^22p^4) - 0.98807(2p^6) + 0.00021(2s^22p^33p) + 0.00633(2p^53p)$$

$$2s^22p^3(^2P)3d\,{}^3F^\circ = -0.18054(2s^22p^3(^2D)3d) + 0.98343(2s^22p^3(^2P)3d) + 0.01650(2s\,2p^4(^1D)3p)$$

$$2p^53p\,{}^3D = 0.13836(2s^22p^3(^2P)3p) - 0.00007(2s^22p^3(^2D)3p) + 0.99038(2p^53p)$$

$$2p^53s\,{}^5S^\circ = 0.99925(2p^53s) + 0.03817(2s\,2p^43p) + 0.00672(2s\,2p^44p)$$

$$2s^22p^3(^2D)3d\,{}^3P^\circ = 0.01047(2s\,2p^5) - 0.01247(2p^53s) - 0.030167(2p^53d) + 0.035667(2s\,2p^43p)$$
$$+ 0.030935(2s^22p^33s) + 0.228099(2s^22p^3(^2P)3d) - 0.97189(2s^22p^3(^2D)3d)$$

$$2s^22p^4\,{}^1S = 0.98809(2s^22p^4) - 0.15386(2p^6) - 0.00191(2s^22p^33p) + 0.00007(2p^53p)$$

$$2s2p^5\,{}^3P^\circ = -0.99992(2s2p^5) + 0.00495(2s^22p^33s) - 0.00538(2s^22p^3(^2P)3d) + 0.00925(2s^22p^3(^2D)3d)$$

$$2s^22p^4\,{}^1D = 0.99850(2s^22p^4) - 0.00055(2s^22p^3(^2P)3p) - 0.05467(2s^22p^3(^2D)3p) - 0.00079(2p^53p)$$

$$2s2p^5\,{}^1P^\circ = 0.99986(2s2p^5) + 0.00476(2p^53s) - 0.01008(2p^53d) = 0.00524(2s^22p^33s)$$
$$- 0.00526(2s^22p^3(^2P)3d) + 0.00957(2s^22p^3(^2D)3d)$$

were carried out by comparing cross sections calculated when either set was used. Insignificant changes in the various $n=2$ and $n=3$ cross sections were obtained. The cross sections presented in this paper were thus obtained using the set-II wave functions, and Table IV gives some examples of the target states used. The complete set of states and configurations used in the calculation of the cross sections is too large to reproduce in full here.

In Table III we list f_L and f_V for some optically allowed transitions. The largest oscillator strengths are for transitions from the $2p$ level to the $3d$ levels. We note that f_L and f_V differ considerably for transitions out of the $2s$ level. For the $2s^2 2p^3 3s\,^3P^\circ$ state, the agreement between f_L and f_V is reasonably good. However, for the inner-shell transitions to the $2s2p^4(^4P)3p\,^3P^\circ$, $2s2p^4(^2P)3p\,^3P^\circ$, and $2s2p^5\,^3P^\circ$, the agreement is poor, even though the same orbitals are used. In order to make f_L and f_V more nearly equal for such transitions one must add many configurations involving higher orbitals. This was also observed for Na-like ions[9] and for Ti^{+3}.[10] In the latter case, it was found that the scattering approximation used was more important than more extensive configuration interaction in the target wave functions for transitions involving inner-shell excitations.

The coupled integro-differential equations were solved using the noniterative integral equation method of Henry *et al.*[13] Step size at small radial distances were chosen to be $0.0017a_0$, and exchange terms were dropped at $17.0a_0$, where the magnitude of the largest orbital had fallen to less than 10^{-3}.

Partial cross sections for the forbidden transitions fall off rapidly with increasing total angular momentum L, and truncation of the partial sum at $L=20$ is sufficient to achieve a cross-section sum accurate to 0.01% at the highest energy considered for most of the transitions. For the $2s^2 2p^4\,^3P-2s2p^5\,^3P^\circ$ cross section values of L up to 40 were retained to converge the sum to within 0.1% at the highest energy. For $L \geq 25$ a unitarized Born approximation was used to obtain the contribution from the highest partial waves. For high L the Bethe partial cross sections were generally within 6% of the close-coupling (CC) cross sections.

The collision strength, $\Omega(i,f)$, for a transition between some initial state i and final state f is related to the cross section σ_{if} by

$$\Omega(i,f)=\omega_i k_i^2 \sigma_{if} \ , \tag{6}$$

where ω_i is the statistical weight of the initial state i, k_i^2 is the energy of the incident electron (in rydbergs) relative to the state i, and the cross section is measured in units of πa_0^2.

III. RESULTS AND DISCUSSION

The cross sections in Fig. 1 were obtained by coupling the states $2s^2 2p^4\,^3P$, $2p^5 3d$, and $2s^2 2p^3 3d$ (3CC) and those in Fig. 8 by coupling the states $2s^2 2p^4\,^3P$, ^1D, $2s^2 2p^3(^2D)3p$, and $2s^2 2p^3(^2P)3p$ (4CC). For the rest of the figures, the states which are indicated in each figure were coupled together along with the ground state in the CC approximation. In Figs. 3 and 5, for example, the cross sections were computed in 7CC and 8CC calculations, respectively. $\sigma_L(\pi a_0^2)$ in Figs. 1 and 2, and $\sigma(\pi a_0^2)$ in Figs. 3—8 represent short forms of σ_L (in units of πa_0^2) and σ (in units of πa_0^2), respectively.

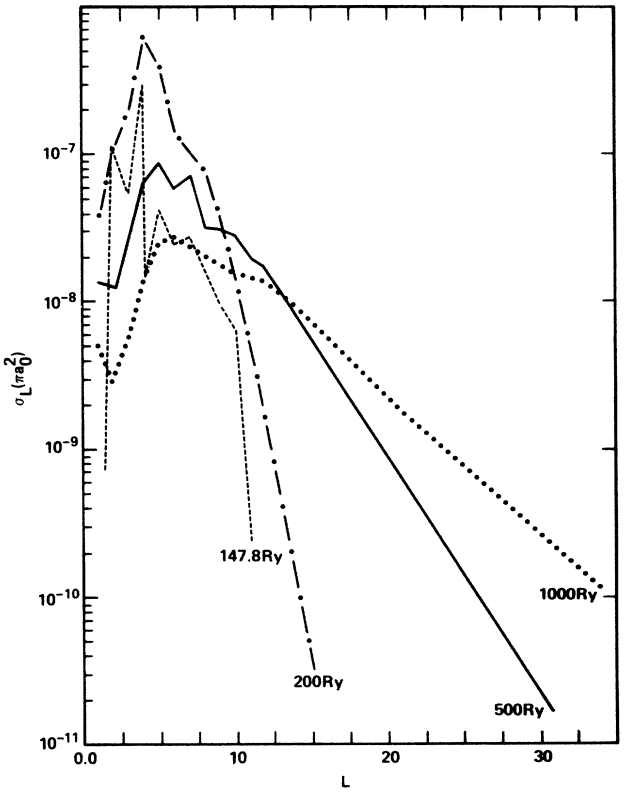

FIG. 1. Partial cross sections as a function of L for the $2s^2 2p^4\,^3P \rightarrow 2s^2 2p^3(^2P)3d\,^3F^\circ$ transition at four collision energies.

In Fig. 1 we show the partial cross sections as a function of L for the $2s^2 2p^4\,^3P \rightarrow 2s^2 2p^3(^2P)3d\,^3F^\circ$ transition at 147.8, 200, 500, and 1000 Ry. At all four energies the partial cross section peaks near $L=5$, but the peak cross section occurs at higher values of L for the higher energies. The peak value of the partial cross section diminishes with increasing energy. At lower energies the contribution from higher partial waves decreases rapidly with increasing L after $L=10$. At higher energies the decrease in σ_L is more gradual.

In Fig. 2, the partial cross sections as a function of L are shown for transition from the ground state to the ^3D states at a collision energy of 350 Ry. Here the peak σ_L occurs near $L=7$ for all three transitions. While σ_L has the same shape for all three transitions, the partial cross sections are much higher at all L for the transition to the $2s^2 2p^3(^2P)3p$ state than for transitions to the other two ^3D states. The values of the total cross sections are $4.24\times10^{-7}\pi a_0^2$, $7.63\times10^{-9}\pi a_0^2$, and $4.85\times10^{-9}\pi a_0^2$ for the $2s^2 2p^3(^2P)3p$, $2s^2 2p^3(^2D)3p$, and the $2p^5 3p$, respectively.

In Figs. 3—8 we show the computed cross sections for several types of transitions. For brevity, a cross section such as $\sigma(2s^2 2p^4\,^3P-2s2p^5\,^3P^\circ)$ is represented in Fig. 5, for example, simply as $\sigma[2s2p^5]$. There should be no

confusion because for each figure the cross sections belong to the same symmetry, except in Fig. 3 which gives cross sections for the $^{3,5}S^{\circ}$ states. However, the $^{5}S^{\circ}$ cross sections are clearly marked in this figure. The largest cross section is for the $2s^2 2p^4\,{}^3P \rightarrow 2s2p^5\,{}^3P^{\circ}$ transition which is approximately $3.2\times10^{-3}\pi a_0^2$ at the lowest collision energy of 26.2 Ry and is still relatively large ($\sim10^{-4}$) at 800 Ry (see Fig. 5). The cross sections for $k^2 \leq 150$ Ry for the $2s2p^5\,{}^3P^{\circ}$ and $2s2p^5\,{}^1P^{\circ}$ states in Figs. 5 and 6, respectively, are from our previous calculation[14] in which only the $n=2$ channels were coupled. The cross section for the transition to the $2s^2 2p^3(^2D)3d\,{}^3P^{\circ}$ is also relatively large. It is about $3.5\times10^{-5}\pi a_0^2$ at 200 Ry and is only slightly smaller ($2.1\times10^{-5}\pi a_0^2$) at 800 Ry. The transition to the $2s^2 2p^3(^2D)3d\,{}^3S^{\circ}$ state also has a cross section of approximately $1.1\times10^{-4}\pi a_0^2$ near 200 Ry and it diminishes slowly over the range of collision energies shown (see Fig. 3).

In order to investigate the effects of coupling among the terms of the ground-state configuration, we first computed the cross section for the $2p^6\,{}^1S$ state with only the $2s^2 2p^4\,{}^3P$ and the $2p^6\,{}^1S$ states in a two-state close-coupling calculation. We then calculated the cross section for this transition with the $2s^2 2p^4\,{}^1D$ and $2s^2 2p^4\,{}^1S$ terms included in a four-state calculation. The same procedure was followed for other states in which the coupling was studied. The effects of coupling among the terms of the ground-state configuration were found to be negligible. We also found that the effects of coupling between the $n=2$ and $n=3$ excited states were generally unimportant.

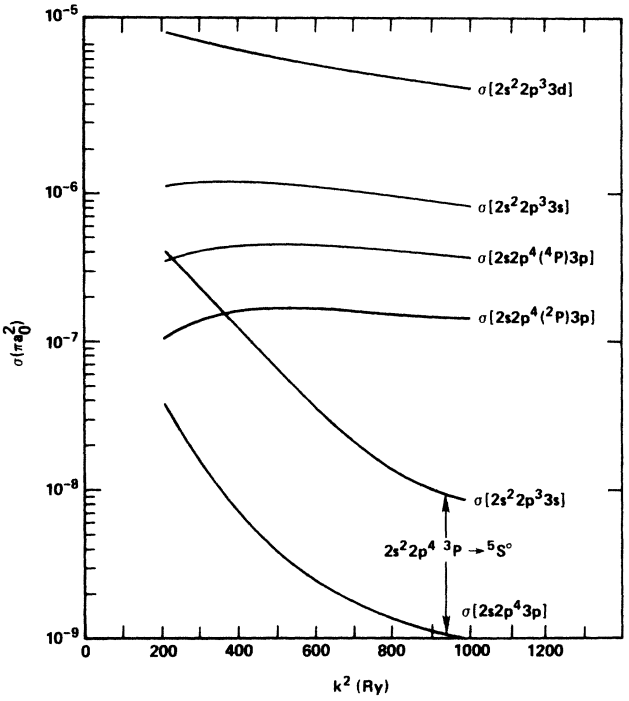

FIG. 3. Cross sections for transition to the $^3S^{\circ}$ and $^5S^{\circ}$ excited states.

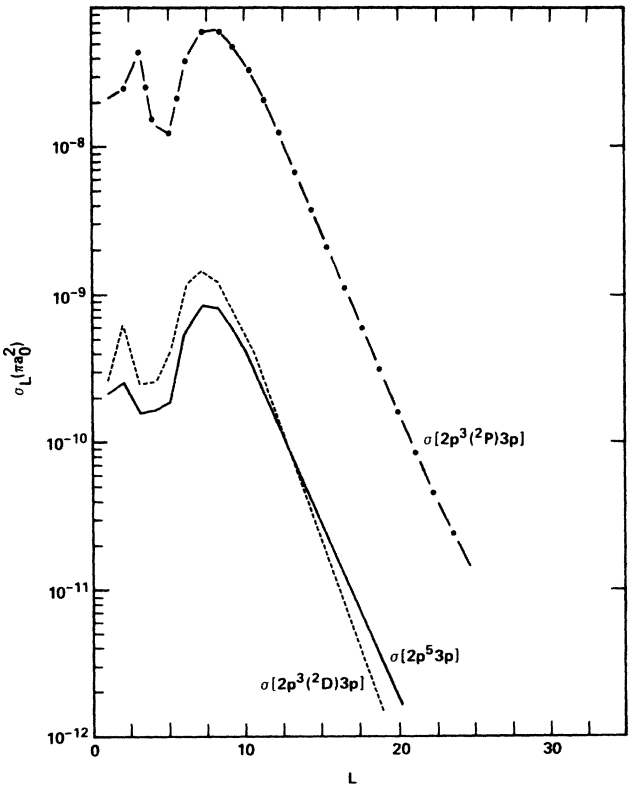

FIG. 2. σ_L vs L at 350 Ry for transition to the ^3D states $2s^2 2p^3(^2D)3p$, $2s^2 2p^3(^2P)3p$, and $2p^5 3p$.

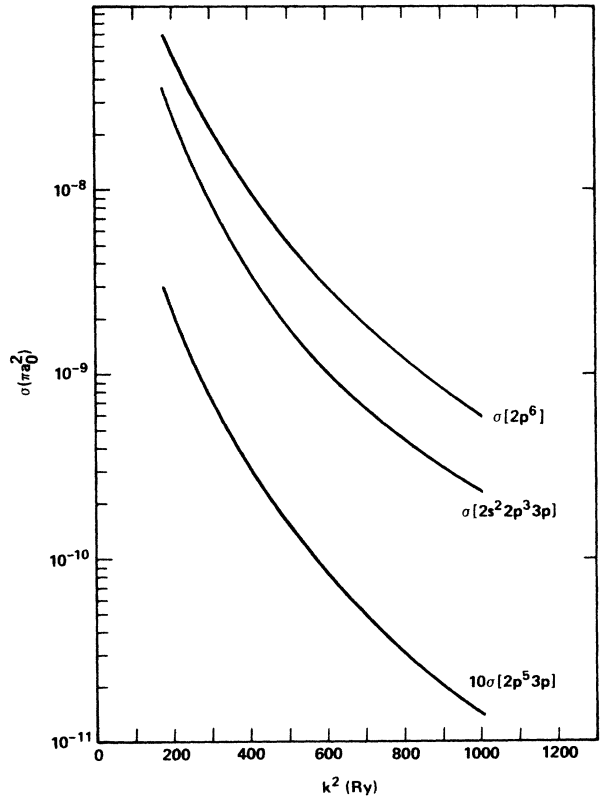

FIG. 4. Cross sections for transition to the ^1S excited states.

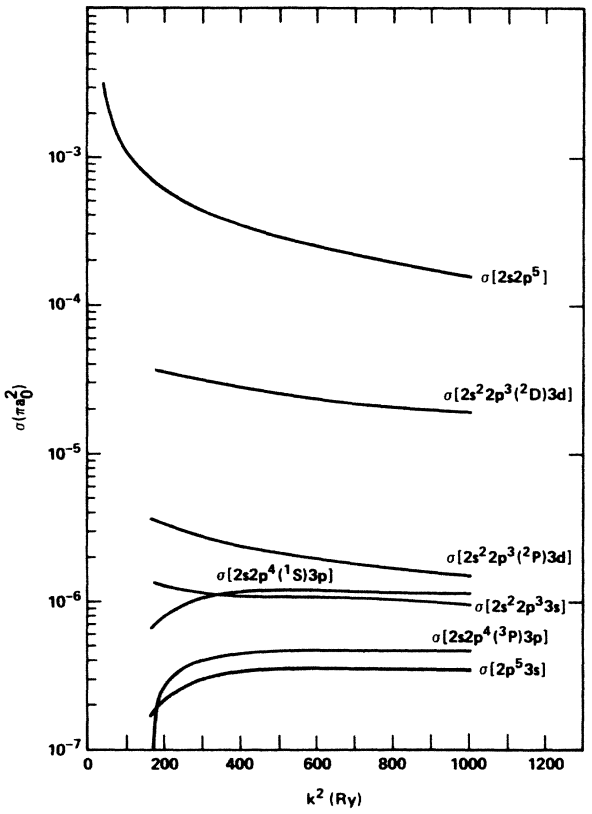

FIG. 5. Cross sections for transition to the $^3P^\circ$ excited states.

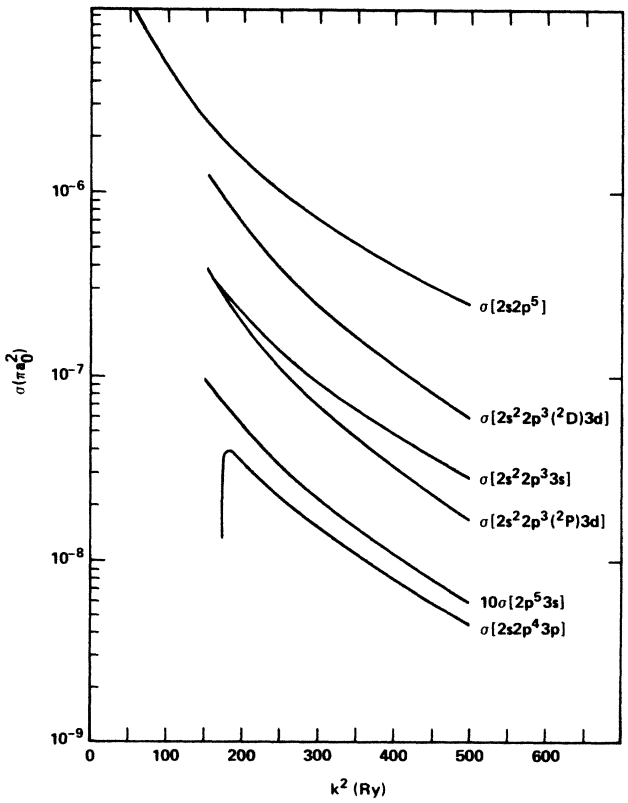

FIG. 6. Cross sections for transition to the $^1P^\circ$ excited states.

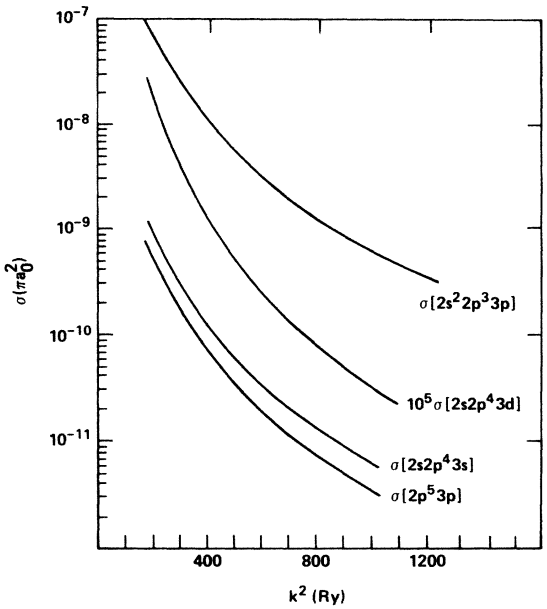

FIG. 7. Cross sections for transition to the ^3S excited states.

A 2CC calculation is expected to give cross sections which are better than 10% of their corresponding multistate close-coupling results when transitions are between the ground state and the $n=3$ configurations. This follows from tests involving comparison of cross sections calculated in 2CC using our CI target wave functions and some of the present multistate results. Weak coupling among the various excitation channels can be expected for highly stripped ions such as oxygenlike krypton since the

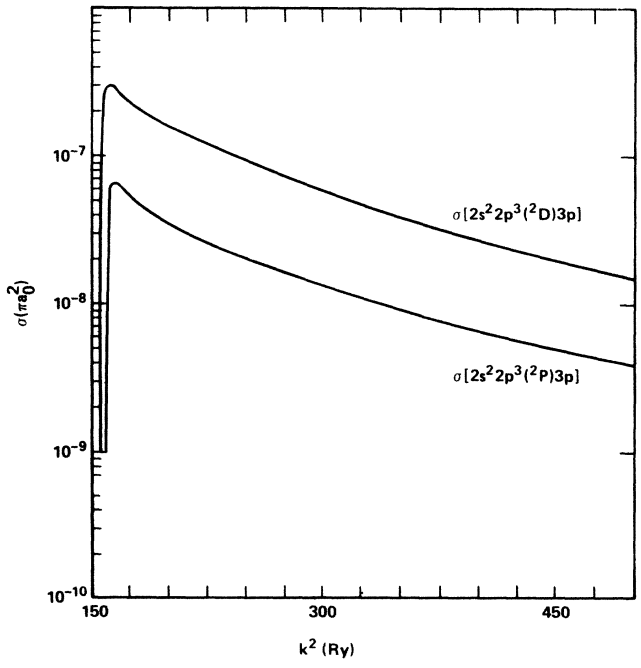

FIG. 8. Cross sections for transition to the ^1D excited states.

Coulomb interaction of the incident electron with the large residual charge on the ion is expected to dominate all other interactions. However, the 2CC approximation is generally inadequate[14] when cross sections between the ground state and the $n=2$ levels are desired.

In the Bethe limit the cross section for a dipole-allowed transition is directly proportional to the oscillator strength and inversely proportional to the transition energy. Consistent with this, our three largest cross sections are for transitions having large oscillator strengths and the largest cross section is for a $\Delta n=0$ transition with a relatively small threshold. Among the transitions to the $n=3$ levels, the largest cross sections are for transitions involving transfer of a $2p$ electron to a $3d$ orbital. In studies of electron impact of neonlike krypton, transitions involving transfer of a $2p$ electron to a $3d$ orbital similarly had large cross sections.[15]

As mentioned in Sec. II, the accuracy of the target wave function and the number of states included in the close-coupling expansion are the two factors having the greatest effect upon the reliability of the calculated cross sections. Near equality of the length and velocity forms of the optical oscillator strengths is often a criterion for gauging the accuracy of the target wave function. We have noted that for certain transitions involving promotion of an inner-shell electron, we did not achieve near equality of f_L and f_V with the wave functions employed in our scattering calculations. Nevertheless, we believe that the target wave functions employed are sufficiently accurate to give reliable results for the calculated cross sections. Burke *et al.*[16] used a ten-state R-matrix expansion to calculate electron-impact excitation of Ti^{+3} from the ground state $3p^6 3d$ to the terms of the $3p^5 3d^2$ configuration. Although there are some sizable differences in the length and velocity forms of the oscillator strengths obtained with their target wave functions, they achieved good agreement with the experimental results of Falk *et al.*[17] Msezane and Henry[10] found that CI target wave functions produced essentially the same cross sections as those obtained using simple Hartree-Fock target wave functions, when used in the close-coupling approximation. Similarly, Henry and Msezane[9] obtained good agreement with measurements of Crandall *et al.*[18] for studies of sodiumlike ions in which an inner-shell $2s$ electron was excited to an autoionizing level.

IV. CONCLUSION

We have used a closed-coupling approximation to obtain electron collision cross sections for selected transition in oxygenlike krypton. We have studied the L dependence of some cross sections and we have studied the effects of couplings among various excitation channels. We found that the effects of these couplings are generally small and for most transitions between the $n=2$ and $n=3$ levels a two-state close-coupling calculation is sufficient for obtaining accurate cross sections. We are currently studying relativistic effects which are being treated as a first-order perturbation to our nonrelativistic wave functions. In future publications we will report the results of these studies along with electron collision strengths in intermediate coupling.

ACKNOWLEDGMENTS

Work was performed under the auspices of the U.S. Department of Energy by Lawrence Livermore National Laboratory under Contract No. W-7405-Eng-48. One of us (R.J.W.H.) was supported in part by the U.S. Department of Energy, Division of Chemical Sciences. Discussions with and suggestions by Dr. A. U. Hazi are appreciated. Generous computer time on the National Magnetic Fusion Energy Computer Center (NMFECC) Cray computers is greatly appreciated by one of us (A.Z.M.).

[1] V. Feldman and G. A. Doschek, J. Opt. Soc. Am. **67**, 726 (1977).
[2] C. Froese Fischer and H. P. Saha, Phys. Rev. A **28**, 3169 (1983).
[3] K. T. Cheng, Y. K. Kim, and J. P. Desclaux, At. Data Nucl. Data Tables **24**, 111 (1979).
[4] B. Edlen, Phys. Scr. **28**, 51 (1983).
[5] D. D. Dietrich, R. E. Stewart, R. J. Fortner, and R. J. Dukart, Phys. Rev. A **34**, 1912 (1986).
[6] A. K. Bhatia and V. Feldman, J. Appl. Phys. **53**, 4711 (1982).
[7] A. Z. Msezane, K. J. Reed, and R. J. W. Henry (unpublished).
[8] R. J. W. Henry, Phys. Rep. **68**, 1 (1981).
[9] R. J. W. Henry and A. Z. Msezane, Phys. Rev. A **26**, 2545 (1982).
[10] A. Z. Msezane and R. J. W. Henry, *Proceedings of the Abstracts of Contributed Papers, Fourteenth International Conference on the Physics of Electronic and Atomic Collisions, Palo Alto, 1985,* edited by M. J. Coggiola *et al.* (North-Holland, Amsterdam, 1985).
[11] E. Clementi and C. Roetti, At. Data Nucl. Data Tables **14**, 177 (1974).
[12] A. Hibbert, Comput. Phys. Commun. **9**, 141 (1975).
[13] R. J. W. Henry, S. P. Rountree, and E. R. Smith, Comput. Phys. Commun. **23**, 233 (1981).
[14] A. Z. Msezane, K. J. Reed, and R. J. W. Henry, Phys. Rev. A **34**, 2540 (1986).
[15] K. J. Reed and A. U. Hazi, LLNL Report NO. UCRL 87014, 1981 (unpublished).
[16] P. G. Burke, W. C. Fon, and A. E. Kingston, J. Phys. B **17**, L733 (1984).
[17] R. A. Falk, G. H. Dunn, D. C. Griffin, C. Bottcher, D. C. Gregory, D. H. Crandall, and M. S. Pindzola, Phys. Rev. Lett. **47**, 494 (1981).
[18] D. H. Crandall, R. A. Phaneuf, R. A. Falk, D. S. Belic, and G. H. Dunn, Phys. Rev. A **25**, 143 (1982).